Positive Receptor Feedback during Lineage Commitment Can Generate Ultrasensitivity to Ligand and Confer Robustness to a Bistable Switch

Santhosh Palani* and Casim A. Sarkar*†
*Department of Bioengineering and †Department of Chemical and Biomolecular Engineering, University of Pennsylvania, Philadelphia, Pennsylvania 19104-6321

ABSTRACT Cytokines and lineage-specific transcription factors are critical molecular effectors for terminal differentiation during hematopoiesis. Intrinsic transcription factor activity is often believed to drive commitment and differentiation, whereas cytokine receptor signals have been implicated in the regulation of cell proliferation, survival, and differentiation. In erythropoiesis, recent experimental findings provide direct evidence that erythropoietin (Epo) can generate commitment cues via the erythropoietin receptor (EpoR); specifically, EpoR signaling leads to activation of the transcription factor GATA-1, which then triggers transcription of erythrocyte-specific genes. In particular, activated GATA-1 induces two positive feedback loops in the system through the enhanced expression of both inactive GATA-1 and EpoR, the latter of which is externally regulatable by Epo. Based upon this network architecture, we present a mathematical model of GATA-1 activation by EpoR, which bidirectionally links a lineage-specific receptor and transcription factor. Our deterministic model offers insight into stimulus-response relationships between Epo and several downstream effectors. In addition to the survival signals that EpoR provides, steady-state analysis of our model suggests that receptor upregulation during lineage commitment can also generate ultrasensitivity to Epo and bistability in GATA-1 activity. These system-level properties can induce a switch-like characteristic during differentiation and provide robustness to the mature state. The topology also suggests a novel mechanism for achieving robust bistability in a purely deterministic manner without molecular cooperativity. The analytical solution of a generalized, minimal model is provided and the significance of each of the two positive feedback loops is elucidated through bifurcation analysis. This network topology, or variations thereof, may link other receptor-transcription factor pairs and may therefore be of general relevance in cellular decision-making.

INTRODUCTION

The process of cellular differentiation entails a complex series of events through which an uncommitted progenitor can morph into a stable specialized cell. Although many of the critical individual molecular components involved in specific differentiation processes have been identified, the complex interactions and topology of signaling and transcriptional networks can lead to nonintuitive behavior. Mathematical modeling and analysis can provide insights into the system-level properties that arise from such an array of interactions.

In cellular processes in which a binary decision must be made, bistability can be an important system-level property that arises from the corresponding signaling networks. Changes in the system input can toggle a bistable system between two steady states; additionally, the system can display memory by sustaining a high (or low) steady-state response after significant reduction (or increase) in the magnitude of the stimulus (1). Biological examples of bistability include cell-cycle regulation in *Xenopus* oocytes (2) and *Saccharomyces cerevisiae* (3), self-sustaining biochemical memory (4), synthetic genetic switches (5–9), and differentiation of common myeloid precursors into macrophages and neutrophils (10). Bistability is often accompanied by ultrasensitivity to a stimulus, another common property of nonlinear systems (11–13). Since, there is growing evidence that cell differentiation is an all-or-none ''switch-like'' event, rather than a continuous transition of an unspecialized cell into a mature one (2,14), mathematical modeling of the commitment process is attractive because the switch-like response and cellular memory implicit in the biological process arise naturally in the formulation of such nonlinear models.

Hematopoiesis, the formation of blood cells, takes place in two distinct stages: primitive differentiation and terminal differentiation. During primitive differentiation, a hematopoietic stem cell differentiates into a multipotent or bipotent progenitor cell, which, upon terminal differentiation, gives rise to a mature cell. It has been suggested that primitive differentiation is primarily a stochastic process involving differential expression of several intrinsic transcription factors, whereas terminal differentiation involves both cell-intrinsic and cell-extrinsic factors (15,16). Lineage-specific cytokines (extrinsic) and transcription factors (intrinsic) are believed to be the important molecular components that affect cell survival, proliferation, and commitment during terminal differentiation.

Erythropoietin (Epo) is a hematopoietic cytokine responsible for the proliferation, survival, and differentiation of erythroid cells (17). The Epo receptor (EpoR) has a single transmembrane domain, an extracellular domain for Epo

Submitted August 24, 2007, and accepted for publication March 21, 2008.

Address reprint requests to Casim A. Sarkar, 240 Skirkanich Hall, 210 S. 33rd St., Dept. of Bioengineering, University of Pennsylvania, Philadelphia, PA 19104-6321. Tel.: 215-573-4072; Fax: 215-573-2071; E-mail: casarkar@seas.upenn.edu.

Editor: Herbert Levine.

0006-3495/08/08/1575/15 $2.00
doi: 10.1529/biophysj.107.120600

binding, and an intracellular domain for signaling (18). In the absence of ligand, Epo receptors exist predominantly as inactive homodimers on the cell surface (19). Binding of Epo to the receptor homodimer changes the orientation of the receptor subunits, which leads to activation of several signaling cascades including the PI3K/AKT, STAT5-Bcl_{XL}, and Ras/MAPK pathways (20). Erythroid progenitors lacking functional EpoR do not mature into erythrocytes and show phenotypic abnormalities (21,22).

The zinc-finger GATA-1 is a transcription factor that plays a critical role in erythroid differentiation (23,24). It binds as a monomer to the consensus sequence (A/T)GATA(A/G), which is present in the promoter and enhancer regions of virtually all erythroid-specific genes (25–28). GATA-1 undergoes several posttranslational modifications (acetylation, phosphorylation, sumoylation, and ubiquitination) that may be critical for its optimal transcriptional activity (29). Analysis of the promoter regions of the EpoR gene shows no TATA or CAAT box, but does reveal the presence of a GATA-1 binding motif, thus providing a meaningful link between a lineage-specific transcription factor and a lineage-restricted receptor (30–32). Active GATA-1 also binds to the regulatory region of its own gene, thereby enhancing its total expression through a positive feedback loop (33–36). Disruption of the GATA-1 gene in murine embryonic stem cells by homologous recombination blocks erythroid development, emphasizing the absolute need for GATA-1 in red blood cell maturation (37).

Common myeloid progenitors give rise to erythroid burst-forming units (BFU-E), the earliest known erythroid precursor cells. BFU-E mature into erythroid colony-forming units (CFU-E); this is accompanied by an increase in EpoR expression and the cells become increasingly dependent on Epo (38,39). EpoR and GATA-1 levels both rise in parallel and reach their maximum during CFU-E maturation into proerythroblasts and their subsequent differentiation into early basophilic erythroblasts (40,41). Both GATA-1 and EpoR levels fall during further maturation from the basophilic stage to the polychromatic stage as cells synthesize large amounts of globins (38,41). Further differentiation from polychromatic erythrocytes to reticulocytes is independent of EpoR and GATA-1, as their levels fall sharply and the cells also show a decrease in globin expression (38,41). Hence, it is during the temporal window from an early CFU-E to a basophilic erythroblast that EpoR and GATA-1 may act in concert to drive commitment of the erythroid precursor to terminal differentiation and induce the synthesis of globins.

Recent evidence suggests several modes of cross talk between EpoR signaling and GATA-1 transcriptional activity, and analysis of these interactions may offer insights into the commitment program during erythroid differentiation. In brief, EpoR signaling via AKT can lead to GATA-1 activation; in return, active GATA-1 can upregulate synthesis of both itself and EpoR (Fig. 1). Epo activates AKT by phosphorylating this kinase at Ser-473 in a PI3K-dependent manner (42). The importance of AKT signaling in erythropoiesis was demonstrated in JAK2-deficient fetal liver progenitor cells: erythroid differentiation can be supported in these cells by overexpressing active AKT and it can also be inhibited by downmodulating AKT using RNA interference (43). Active AKT appears to have a significant role in enhancing GATA-1 transcriptional activity by mediating some of its posttranslational modifications, including phosphorylation and acetylation. AKT phosphorylates GATA-1 at Ser-310 and enhances its transcriptional activity in primary fetal liver cells (42). However, mice with a S310A mutation in GATA-1 showed no hematopoietic abnormalities during normal or stress erythropoiesis, indicating that phosphorylation of GATA-1 is dispensable for red blood cell differentiation and may only be required for maximal activity (44).

p300 and CREB binding protein (CBP) acetyltransferases acetylate GATA-1 at lysine residues present in the C-terminal tail of its zinc fingers (45–47). In vivo chromatin immunoprecipitation assays show that lysine to alanine mutations at the acetylation residues dramatically impair GATA-1 association with chromatin (48), suggesting that acetylation is critical for GATA-1-mediated gene expression. p300 and CBP also have histone acetyltransferase (HAT) activity and may play a role in enhanceosome stability by acetylating GATA-1 and histones (49,50). AKT phosphorylates p300 at Ser-1834 and this has been shown to be essential for AT, HAT, and transcriptional activity of p300 (51–53). Interestingly, Ser-1834 lies in the E1A binding domain that is necessary for binding of p300/CBP to GATA-1 (45). It has also been suggested that phosphorylation may aid in GATA-1 binding to CBP, since the Ser-310 residue of GATA-1 is within the C-terminal acetylation motif of GATA-1 (42). Taken together, these results suggest an additional role for Epo (other than providing survival and proliferation cues) in erythroid precursor commitment and differentiation by activating GATA-1 through the PI3K/AKT pathway and influencing the intrinsic signals that lead to commitment and differentiation.

Based on this experimental evidence, we present a deterministic model of the upregulation and activation of the erythrocyte-specific transcription factor GATA-1, a ''master regulator'' of erythrocyte commitment. Lineage specification models previously reported suggest that erythrocyte differentiation from erythroid/myeloid bipotent precursor can arise due to the differential expression of antagonistic transcription factors (upregulation of GATA-1 and downregulation of PU.1) driven primarily by cell-intrinsic events (54,55). These models provide insight into the dynamics of a binary cell-fate decision from the viewpoint of ''multilineage priming'', auto-stimulation, and reciprocal repression.

The work presented here focuses on erythrocyte commitment rather than differentiation, and examines how both intracellular and extracellular factors may influence the cell-fate decision. As depicted in Fig. 1, the topology of our model captures the essential elements of outside-in signaling (Epo-mediated activation of GATA-1), intracellular signal

amplification (GATA-1-mediated upregulation of GATA-1 synthesis), and inside-out signaling (GATA-1-mediated upregulation of EpoR). Using this model, we show that upregulation of EpoR in erythroid precursor cells upon Epo addition can generate ultrasensitivity to ligand as well as robust bistability in GATA-1 expression during commitment, and this may provide ''switch-like'' differentiation characteristics.

Further analysis of a generalized minimal model confirms that the topological connectivity of the two feedback loops alone is both necessary and sufficient for generating the overall system dynamics. Although there are several ways of achieving bistability (1,56), feedback loops are the most commonly identified mechanism; however, feedback loops that give rise to robust bistability in purely deterministic models have, to date, been shown to be highly cooperative in at least one reaction (57–60). Here, we present what we believe is a novel way of achieving robust bistability in cell signaling networks without molecular cooperativity through two linked positive feedback loops. This topology may have general implications for cellular decision-making.

MODEL DEVELOPMENT

Model construction and description

The core reaction of the proposed erythrocyte commitment model is the activation of GATA-1 by AKT through EpoR signaling (Fig. 1, *light gray background*). Our model concentrates exclusively on the two positive feedback loops that serve to increase the concentrations of the reactant species (AKTpp and GATA-1) in this core reaction, which leads to greater accumulation of GATA-1*, the activated form of a ''master regulator'' of erythrocyte-specific genes. The model specifically incorporates the following components/motifs in the feedback loops that may have an effect on the overall system behavior:

1. EpoR homodimerization. Unlike many other cytokine-receptor systems, EpoR homodimerizes (but does not signal) before Epo addition, which should therefore confer ultrasensitivity to the number of receptor dimers available to bind Epo (19,20). This effect was modeled as a two-step process of EpoR binding to JAK2 and EpoRJ dimerizing to form EpoRJD. Alternatively, EpoR homodimerization could be treated as a single-step process without considering the effect of JAK2.
2. PI3K/AKT pathway. Signaling in the MAPK cascade has been shown to convert graded signals into ultrasensitive responses (61); therefore, the similar cascade structure in the PI3K/AKT pathway might ultrasensitize the signals from the cell surface to GATA-1.
3. Double phosphorylation of AKT. Recent reports have shown that bistability in signaling circuits can arise from multisite phosphorylation (56); hence, we explicitly modeled AKT activation as two phosphorylation steps.
4. Transcription and translation. Delay in feedback loops has been shown to generate interesting behaviors in signaling networks (62), so these two processes were modeled as separate steps. Additionally, explicit inclusion of mRNA species in the model facilitates comparisons with experimental microarray data (see the Supplementary Material, Fig. S1, Data S1).

We have used a deterministic, ordinary differential equation-based approach to model this signal transduction/transcriptional network. Although this modeling framework represents an ideal approximation of the true intracellular milieu (63), it can still provide useful information regarding the system dynamics, particularly for nonlinear systems of the type studied here (64). In step 1 in Fig. 1, JAK2 binds to the intracellular domain of EpoR to form a receptor-JAK complex (EpoRJ). EpoRJ dimerizes to form EpoRJD in step 3. EpoRJ and EpoRJD undergo constitutive receptor endocytosis (steps 2 and 4). In step 5, Epo binds to the extracellular domain of EpoRJD, forming the activated complex (EpoRJD*) and the endocytosis of the complex is shown in step 6. PI3K is activated (PI3K*) by the complex and is deactivated by a phosphatase (steps 7 and 8). PI3K* converts PIP_2 to PIP_3 in step 9. PIP_3 binds to the PH domain of AKT and phosphorylates AKT on Ser-473 and Thr-308 (steps 11–15). This doubly phosphorylated form of AKT (AKTpp) catalyzes the activation of GATA-1 (step 16). Activated GATA-1 (GATA-1*) is deactivated and degraded in steps 17 and 26, respectively. Monomeric GATA-1* enhances transcriptional synthesis of nuclear EpoR mRNA (EpoRmRNAn) and GATA-1 mRNA (GATA1mRNAn) in steps 18 and 19. The nuclear mRNAs (EpoRmRNAn and GATA1mRNAn) are translocated to the cytoplasm (EpoRmRNAc and GATA1mRNAc, respectively), where they are either translated to their corresponding protein forms or degraded (steps 20–25).

EpoR and GATA-1 are present at basal levels in progenitor cells before the addition of Epo. The basal expression of Epo receptor may be independent of GATA-1 as there is also a Sp1 binding site on the 1.7 kb 5′-flanking region of the EpoR gene (31). Based on current evidence, it appears that, as EpoR is transported to the cell membrane, it is rapidly bound by JAK2 and homodimerizes (19,20). Accordingly, we have assumed 90% of EpoR to be initially present in the dimeric state, 9% to be monomers bound by JAK2, and 1% to be free receptors. Activation and deactivation reactions of PI3K, PIP_2, GATA-1, and AKT are assumed to have Michaelis-Menten kinetics. AKT phosphorylation is modeled as a two-step process (65). Double phosphorylation of AKT by 3′-phosphoinositide-dependent protein kinase 1 (PDK1) is necessary for its complete activation (66,67). Dephosphorylation of PI3K*, PIP_3, and AKTpp are implicitly modeled without considering the rate of change of the phosphatases involved. The role of AKTpp in GATA-1 activation is modeled as a single enzymatic step, encompassing both

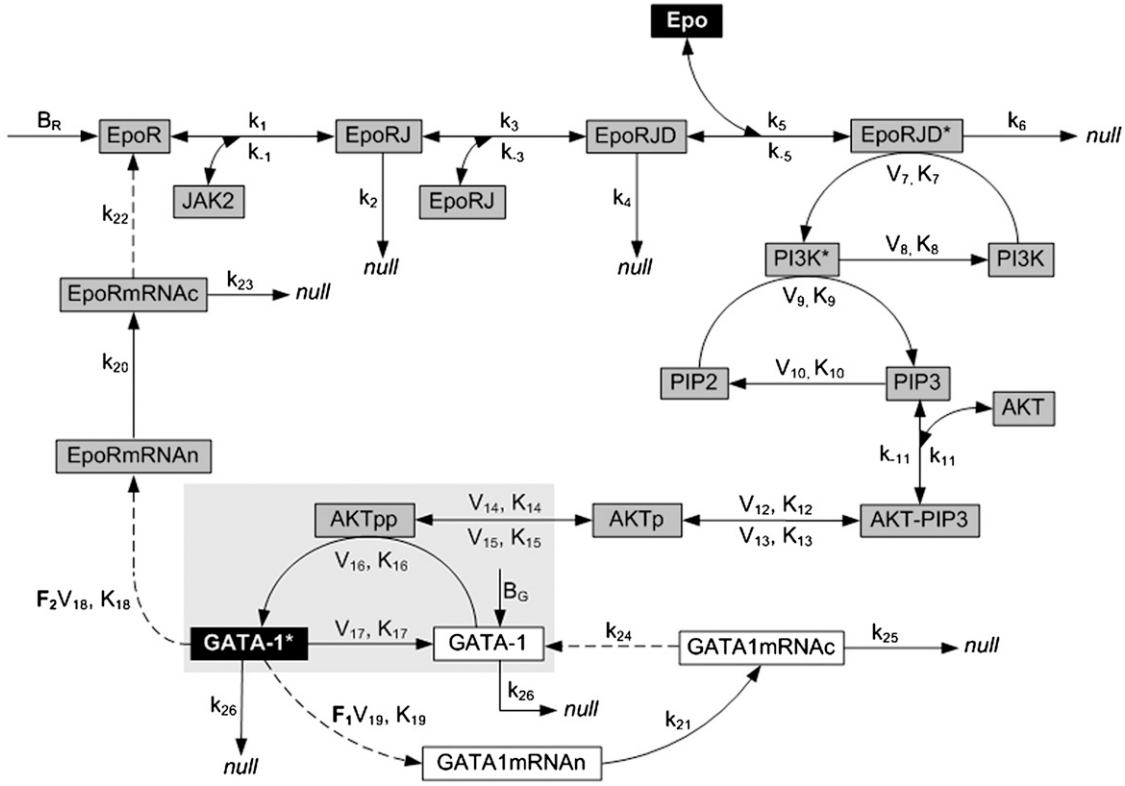

FIGURE 1 Kinetic model of the EpoR/GATA-1 network implicated in erythrocyte progenitor commitment. EpoR and GATA-1 are present at low basal levels before the addition of Epo. Epo binds to EpoR homodimers (EpoRJD), thereby activating AKT through the PI3K/AKT pathway. Doubly phosphorylated AKT (AKTpp) activates GATA-1 directly and indirectly through covalent modifications (modeled here as a single step). GATA-1*, the activated form of the transcription factor, upregulates GATA-1 and EpoR gene expression by binding to GATA motifs present in the response elements of their corresponding genes. The core reaction of the model is the activation of GATA-1 by AKTpp and is highlighted with a light gray background. The reactants in the open boxes comprise one feedback process (with transcriptional strength F_1), a synthesis loop that generates more inactive GATA-1 (substrate), and the species in the dark gray boxes represent a second feedback process (with transcriptional strength F_2), an Epo-regulated loop that makes more AKTpp (enzyme). Both feedback loops provide inputs to the core reaction to form GATA-1* (product). All reactants except Epo and JAK2 are time variant. Reaction sets (1–6, 11, 20, 21, 23, 25, and 26), (7–10, 12–17, 22, and 24), and (18 and 19) are modeled with mass-action, Michaelis-Menten, and rapid-equilibrium kinetics, respectively. The species names ending with mRNAc and mRNAn denote cytoplasmic and nuclear mRNA, respectively. Double-headed and single-headed solid arrows indicate reversible and irreversible reactions respectively. Dashed arrows specify irreversible reactions (transcription, translation) in which reactants are not consumed. *, p, and pp denote the activated, singly phosphorylated, and doubly phosphorylated forms of species. All reactions going to *null* denote first-order degradation processes. The values of the rate constants shown in the figure are given in the Supplementary Material, Table S5 (Data S1).

direct (e.g., phosphorylation) and indirect (e.g., acetylation) mechanisms. It is important to note that Epo may activate GATA-1 by AKT-independent mechanisms, but this does not change the qualitative nature of the model (see minimal model below). The mRNA transcription rate is assumed to saturate hyperbolically with active transcription factor concentration, a rapid-equilibrium approximation (68). The rate of translation is approximated to be proportional to the concentration of the cytoplasmic mRNA (69). All degradation reactions are modeled with first-order kinetics.

Positive feedback loops

There are two feedback loops considered in this model. Since GATA-1* positively autoregulates its own transcriptional rate, reactions 19, 21, and 24 drive the first positive feedback loop. This loop increases the concentration of inactive GATA-1 in the cell. The strength of this feedback is governed by the parameter F_1V_{19}, the maximal transcriptional rate of the GATA-1 gene, shown in reaction 19. GATA-1* is also shown to regulate the synthesis rate of EpoRJD through reactions 18, 20, 22, 1, and 3, which start the second positive feedback loop, whose strength is denoted by F_2V_{18}, the maximal rate of production of EpoR mRNA. In this loop, GATA-1* upregulates the expression of EpoRJD, which in turn increases the number of complexes formed on the cell surface and leads to the increase in the concentration of activated AKT kinase (AKTpp). In this model, F_1 and F_2 determine the relative strengths of the feedback loops as V_{18} and V_{19} are kept equal and constant. The core reaction in the model is the activation of GATA-1 by AKTpp (reaction 16) and the two feedback loops work synchronously to drive this reaction and produce GATA-1*, which in turn drives both of the feedback loops and also regulates the transcription of other erythrocyte specific genes.

Nondimensionalization and computation

The full model, which consists of 18 ordinary differential equations derived from 27 reactions with 44 parameters, is given in the Supplementary Material (Table S1, Data S1). To simplify parameter estimation and mathematical analyses, the model was completely nondimensionalized; the nondimensional forms of the differential equations and the parameters are also given in the Supplementary Material (Tables S2 and S3, respectively, Data S1). In the nondimensional model, each reactant concentration is normalized by the total concentration of its respective basal inactive form. The species used in the mathematical analyses are Epo receptor homodimer (EpoRJD), complex (EpoRJD*), activated AKT (AKTpp), and activated GATA-1 (GATA-1*). The respective nondimensional forms of these reactants are

$$[\mathrm{RJD}] = \frac{[\mathrm{EpoRJD}]}{[\mathrm{EpoR_T}]_0}, \quad [\mathrm{C}] = \frac{[\mathrm{EpoRJD^*}]}{[\mathrm{EpoR_T}]_0},$$
$$[\mathrm{App}] = \frac{[\mathrm{AKTpp}]}{[\mathrm{AKT_T}]}, \quad [\mathrm{GA}] = \frac{[\mathrm{GATA\text{-}1^*}]}{[\mathrm{GATA\text{-}1_T}]_0}.$$

A complete list of the nondimensional reactants and their initial conditions is provided in Table S4 in the Supplementary Material (Data S1). The nondimensional equations were solved using the Systems Biology Toolbox (SBtoolbox) for MATLAB (The MathWorks, Natick, MA) (70). Parameter sensitivity and parameter estimation were also performed with SBtoolbox. MATLAB was used for analyzing bistability and ultrasensitivity through steady-state response plots.

Parameter estimation and sensitivity analysis

Of the 44 parameters present in the model, 29 parameters were incorporated directly from the literature, 8 parameters were refined from values provided in the literature, and the remaining 7 parameters (V_{16}, K_{16}, V_{17}, K_{17}, F_1, F_2, k_{26}) were estimated to fit time course measurements of GATA-1 DNA binding activity during erythroid precursor commitment and differentiation as reported by Dalyot et al. (41). Of these 7 parameters, the steady-state values of the reactants in the model are highly sensitive only to F_1, F_2, and k_{26}. To initially compare the model to these experimental data, a negative feedback loop was added to account for the degradation of GATA-1* after progenitor commitment. This was necessary since the experimental data cover a much broader temporal window of the differentiation process, from GATA-1* production in progenitors to complete GATA-1 degradation in mature erythrocytes. We have assumed that the change in GATA-1 DNA binding activity is due to corresponding changes in the levels of GATA-1*. The fitted parameters were then used in mathematical analyses performed without the negative feedback loop, as our model is only intended to analyze the commitment decision of the progenitor cells much earlier in the differentiation process and not account for larger-scale phenotypic changes that are observed in mature erythrocytes after commitment. Tables S5 and S6 (Data S1) give the values of the estimated parameters and the initial conditions of the reactants in the model. Parameter sensitivity analysis was performed for the Epo receptor dimer, complex, activated AKT, and activated GATA-1 by perturbing all 44 parameters and obtaining the normalized steady-state sensitivities (ranging from 0 to 1). The most sensitive parameters for each of the reactants are given in Fig. S2 (Data S1).

To further validate this fully parameterized EpoR/GATA-1 model (including the negative feedback loop), it was used to perform kinetic simulations of total (nuclear + cytoplasmic) EpoR and GATA1 mRNA levels. These simulations were then compared to experimental measurements of EpoR and GATA-1 mRNA levels (71), which were obtained from the NCBI Gene Expression Omnibus (GEO) database (No. GDS2431) and which represent experimental data entirely independent from those used for parameter fitting. The comparison of model and experiment is given in Fig. S1 (Data S1) and suggests that the model is capable of making accurate predictions.

Identification of a generalized minimal model

To ascertain what topological features in the EpoR/GATA-1 model are responsible for its robust bistability, the model was systematically reduced to a minimal form by stepwise elimination of various linear topological motifs, including EpoR homodimerization, PI3K/AKT cascading, multisite phosphorylation, and individual transcription and translation steps (data not shown). Conversely, both feedback loops were critical for robust bistability (see Results).

The minimal model (see Fig. 6) consists of the following reactions. The cell-surface receptor and the inactive lineage-specific transcription factor (InactiveTF) are expressed at basal (ligand-independent) levels in the naïve cell. After addition of ligand, a fraction of the cell-surface receptors become complexes (step 2) and transmit a downstream signal to enzymatically activate the transcription factor (step 4). Constitutive receptor endocytosis, complex internalization, and InactiveTF degradation reactions are shown in steps 1, 3, and 8, respectively. The active transcription factor (ActiveTF) can then upregulate the expression of both receptor and inactive transcription factor (steps 6 and 7, respectively). ActiveTF can be deactivated or degraded (steps 5 and 9, respectively). The activation of transcription factor by complex and its deactivation are modeled as single enzymatic steps and are assumed to have Michaelis-Menten kinetics. Complex internalization and all degradation reactions are modeled to have first-order kinetics. The transcription and translation reactions are modeled as a single step, where the rate of protein formation is assumed to saturate hyperbolically with the concentration of active transcription factor. The state of the system is represented by the concentration of ActiveTF; high levels denote the on-state (committed state) and low levels denote the off-state (naïve state).

Nondimensionalization and computation of the minimal model

The dimensional and nondimensional forms of the minimal model, each consisting of four differential equations, are provided in the Supplementary Material (Tables S7 and S8, Data S1). The species present in the minimal model are ligand (L, time invariant), receptor (R), complex (C), inactive transcription factor (ITF), and active transcription factor (ATF). The nondimensionalization was performed in a manner analogous to the EpoR/GATA-1 model (Tables S9 and S10, Data S1):

$$[\mathrm{L}] = \frac{[\mathrm{Ligand}]}{\mathrm{K_d}}, \quad [\mathrm{R}] = \frac{[\mathrm{Receptor}]}{[\mathrm{Receptor}]_0}, \quad [\mathrm{C}] = \frac{[\mathrm{Complex}]}{[\mathrm{Receptor}]_0},$$
$$[\mathrm{ITF}] = \frac{[\mathrm{InactiveTF}]}{[\mathrm{InactiveTF}]_0}, \quad [\mathrm{ATF}] = \frac{[\mathrm{ActiveTF}]}{[\mathrm{InaciveTF}]_0}.$$

The system of differential equations was solved analytically using Maple (Maplesoft, Waterloo, Canada) and the full solution for all reactants is given in the Supplementary Material (Table S11, Data S1). Bistability and bifurcation analyses were performed using MATLAB. Parameter sensitivity analysis was performed using SBtoolbox. The most sensitive parameters for each reactant are provided in Fig. S3 and the values of the kinetic parameters in this model are given in Table S12 (Data S1).

RESULTS

Bistability and ultrasensitivity in the EpoR/GATA-1 network

Stimulus/response plots have been used to predict bistability, hysteresis, and ultrasensitivity in molecular networks (2,5). The system is induced over a wide range of input stimuli and the corresponding responses are obtained after the system reaches steady state. The state of our EpoR/GATA-1 network is represented by the concentration of GATA-1*; high levels (obtained from both accumulation and activation of GATA-1) denote the on-state (committed state) and low levels denote the off-state (uncommitted state). In these simulations, Epo was considered to be the stimulus, and the responses of important downstream effectors activated by the ensuing signals were analyzed. In Fig. 2, the steady-state values of the nondimensionalized reactants (RJD, C, App, GA) are plotted against the concentration of Epo normalized to its dissociation constant (K_d = 58 pM (72)). When [Epo] = 0, the system is in the off-state, with RJD at its basal steady-state value of 0.45, and C, App, and GA all at zero, as there are no complexes. As the Epo concentration increases from 0, the steady-state value of the Epo receptor dimer decreases (Fig. 2 *A*) as a result of complex formation (Fig. 2 *B*) and there is a subsequent marginal increase in App and GA (Fig. 2, *C* and *D*). As the concentration of Epo is further increased to 0.96 K_d, the number of complexes formed increases, but this is still not sufficient to maintain the positive feedback loops and the system remains in the off-state. Only when the input stimulus exceeds 0.96 K_d does the system switch to the on-state, as the complexes can then generate enough AKTpp for GATA-1* levels to exceed the threshold concentration needed to sustain the feedback loops. Therefore, the system exhibits ultrasensitivity for a small perturbation in the concentration of Epo about 0.96 K_d. The on-state is accompanied by a large burst of GATA-1*, an event known to precede the accumulation of various erythroid specific genes (41). The system continues to remain in the on-state with further increase in Epo levels.

To explore whether this network can exhibit memory, the system was taken to the on-state by increasing the concentration of Epo to its K_d value. The stimulus was then reduced to 0.96 K_d and the system was allowed to reach steady state. It can be seen from the plots that the system remains in the on-state as the active positive feedback loops can sustain the system in the committed state. Thus, the downstream effectors in the system exhibit hysteresis with respect to cytokine stimulus. As the Epo concentration is further reduced from 0.96 K_d to 0.008 K_d, the steady-state value of RJD increases since less complexes are formed and, in turn, there is a reduction in the levels of App; nonetheless, the number of complexes is still sufficient to sustain the feedback loops and to maintain high levels of GATA-1*. As Epo levels are reduced below 0.008 K_d, the system switches back to the off-state due to a lack of sufficient Epo-mediated signaling. When the system is in the committed state, removal of the stimulus below the threshold level does not immediately bring the system back to the off-state, instead exhibiting bistability over a large range of stimulus concentration. This bistable expression of GATA-1* can reduce the sensitivity of the system to noise by necessitating a high Epo concentration to initially achieve the on-state and, thereafter, by providing marked robustness to the active state. Though the on-state is still maintained when the stimulus level is reduced ~120-fold below the threshold concentration, further decreases in Epo concentration drive the system back to the off-state, suggesting that it is not completely irreversible. This is in accord with the phenotypic change observed after commitment during which the cell becomes increasingly independent of EpoR signaling and GATA-1 levels start to fall. The high expression of GATA-1 achieved by Epo induction at commitment can initiate chromatin rearrangements and expression of lineage specific genes, thereby ''locking'' the cell in the mature state. The steady states plotted in Fig. 2 are only the stable values; the unstable steady states are omitted, as they are not experimentally accessible.

Pretreatment can change the threshold concentration of the stimulus

The steady-state response plot of GA (Fig. 2 *D*) shows that the Epo concentration has to be >0.96 K_d for the system to be in the on-state. Is there a way to attain the on-state for values

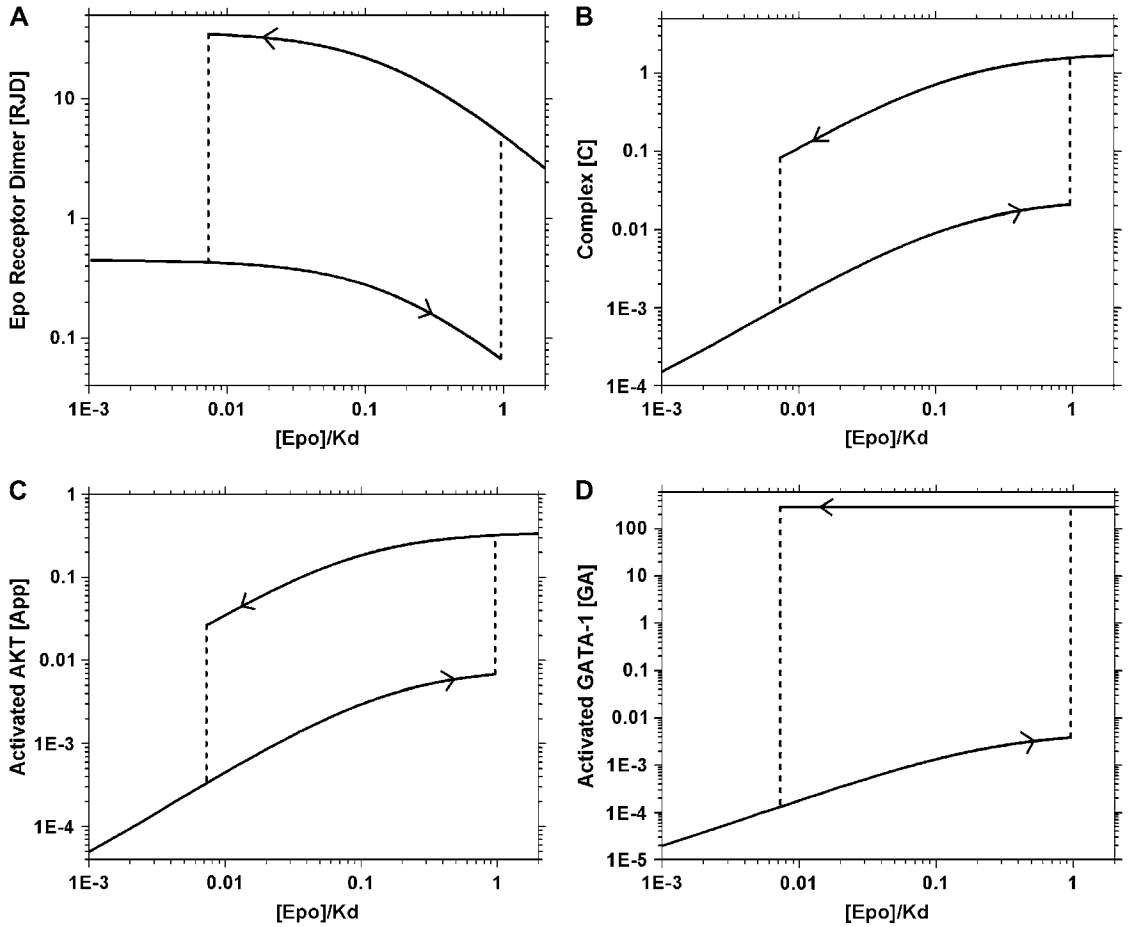

FIGURE 2 Nondimensionalized steady-state response plots: (*A*) Epo receptor dimer [RJD]. (*B*) Epo-Epo receptor complex [C]. (*C*) Activated AKT [App]. (*D*) Activated GATA-1 [GA]. The stimulus, Epo, is normalized to its K_d value and each downstream effector is normalized to the total concentration of its respective basal inactive form. The plots show that, for the fitted values of F_1 (0.04) and F_2 (0.123), the system is ultrasensitive to Epo and exhibits bistability for a wide range of Epo concentrations (0.008–0.96 K_d).

of Epo less than the threshold concentration? Given the memory implicit in this network, we hypothesized that transient pretreatment of cells with high concentrations of Epo should influence their commitment decision since the switch to the on-state is determined by the number of complexes needed to sustain the positive feedback loops. If the cell were pretreated with a high concentration of Epo for a fixed amount of time, it should still be possible to achieve the on-state even if the Epo concentration was then reduced to a level lower than the threshold concentration (0.96 K_d), since there would be an appropriate accumulation of multiple activated species during pretreatment. To test this using our model, the concentration of Epo during pretreatment was fixed at its K_d value and was then reduced to the value given on the *x* axis in Fig. 3. The minimum pretreatment time required for the system to attain the on-state for a range of constant Epo concentrations lower than the threshold concentration is plotted in Fig. 3. The corresponding plots of RJD, C, App, and GA requirements to achieve the on-state for lower Epo concentrations are similar and are given in the Supplementary Material (Fig. S4, Data S1). For Epo concentrations >0.96 K_d, the threshold concentration, the cell does not require pretreatment for commitment. As the Epo concentration is reduced from 0.96 K_d to 0.008 K_d (a range that corresponds precisely to the bistable window in Fig. 2), the pretreatment time required to accumulate sufficient GATA-1* to attain the on-state increases exponentially. Reducing the Epo concentration below 0.008 K_d, does not bring the system to the on-state for any pretreatment time, as the system is in the monostable off-state below this Epo concentration (see Fig. 2).

Double positive feedback loops lead to robust bistability

The EpoR/GATA-1 network consists of two positive feedback loops that coordinate to create a burst of GATA-1*, an event critical for erythrocyte commitment. The first feedback loop is the transcription of *GATA1* by GATA-1*, which increases the concentration of inactive GATA-1 (substrate),

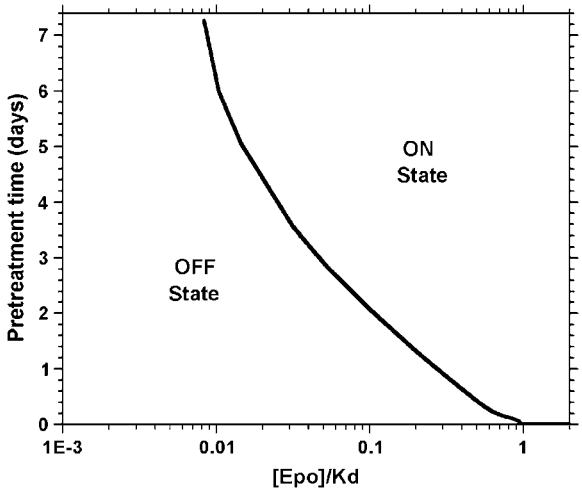

FIGURE 3 Minimum pretreatment time required for the system to attain the on-state for a range of Epo values lower than the threshold concentration (0.96 K_d). Epo is normalized to its K_d. The pretreatment concentration of Epo is kept at its K_d value and is thereafter reduced to the value given on the x axis. The plot suggests that for Epo concentrations >0.96 K_d, the cell should not require pretreatment and, for values less than the threshold concentration, the pretreatment time increases dramatically with decreases in Epo concentration. For Epo values <0.008 K_d, the system will always remain in the monostable off-state for any pretreatment time (cf. Fig. 2).

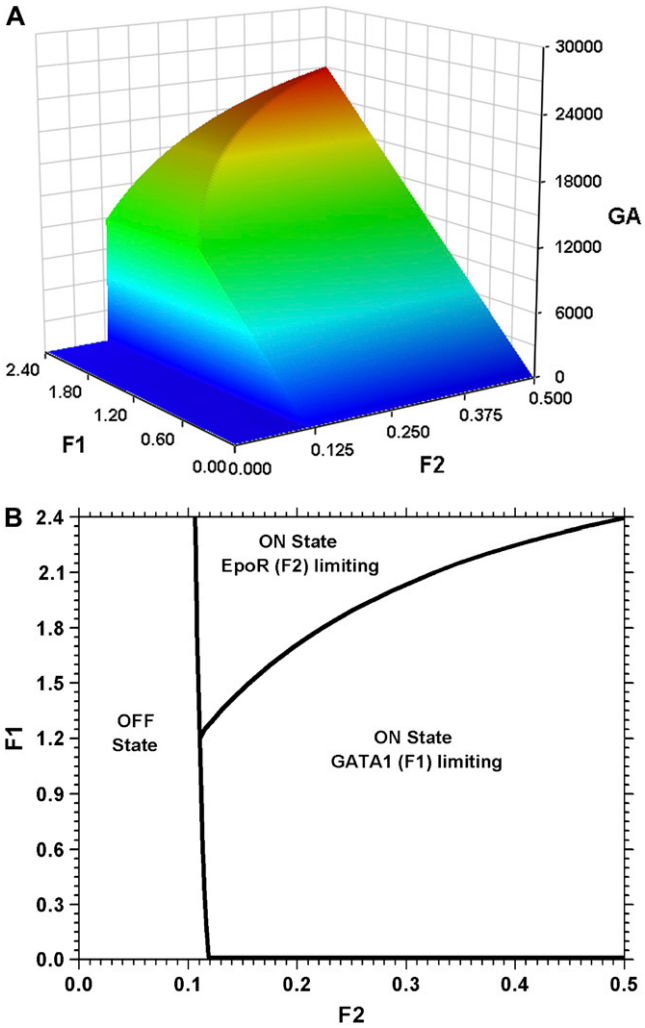

FIGURE 4 Effect of the two positive feedback loops on the on-state GA value. (*A*) Steady-state GA values as a function of F_1 and F_2; Epo is kept at its K_d value. For the estimated values of F_1 (0.04) and F_2 (0.123), the system is strongly F_1-limited. (*B*) Corresponding phase diagram of the 3D plot showing the off-state region, the F_1-limited on-state, and the F_2-limited on-state. Increasing the values of F_1 and F_2 increases the on-state set point of GA in the F_1-limited and F_2-limited regions, respectively. The EpoR/GATA-1 system is likely to behave as an F_1-limited system due the high GA values required to be F_2 limiting.

and the second feedback loop is the transcription of *EPOR* by GATA-1*, which leads to an increase in the levels of AKTpp (enzyme) in the presence of Epo. Parameters F_1 and F_2 govern the maximum transcriptional rates of *GATA1* and *EPOR*, respectively, and hence represent the strength of the GATA-1*/GATA-1 and GATA-1*/EpoR/AKTpp feedback loops, respectively. The parameter-fitted values of F_1 and F_2 are 0.04 and 0.123, which correspond to a steady-state value of GA = 295 as seen in Fig. 2 *D*. In addition to other epigenetic factors, one possible explanation for the difference in the transcriptional rates of *GATA1* and *EPOR* could be the distinct mechanisms by which GATA-1 binds to its consensus sequence present in the promoter regions of these genes (32,34)). It should be noted that the two positive feedback loops are interdependent (linked via the GATA-1 activation reaction; reaction with *light gray background* in Fig. 1) and are necessary for the commitment decision to accumulate GATA-1*. When $F_1 = 0$, the cell cannot make more inactive GATA-1, and can only activate the existing low levels of GATA-1, so the system stays in the off-state for any value of $F_2 > 0$; similarly, when $F_2 = 0$, the cell cannot make enough surface complexes to activate GATA-1 via AKTpp, so the system remains in the off-state for any physiologically reasonable value of $F_1 > 0$. For very large values of F_1, however, high levels of GATA-1* can be achieved, albeit in a manner that does not impart memory to the system (the stimulus/response plot in this case is hyperbolic and monostable everywhere).

Fig. 4 *A* shows a three-dimensional (3D) plot of the steady-state value of GA as a function of F_1 and F_2 when the Epo concentration is equal to its K_d. Changing the values of F_1 and F_2 can switch the system from the off-state to the on-state as well as change the set point of the reactants—specifically GA—in the on-state. As seen from the plot; if either F_1 or $F_2 = 0$, the system is always in the off-state, regardless of the strength of the other feedback process. For the estimated value of $F_1 = 0.04$, as we increase F_2 from 0, the system remains in the off-state until F_2 reaches 0.118. Any increase of F_2 over 0.118 causes the system to switch to the on-state with a GA set point value of 295. Further increasing F_2 does not change the value of GA and the system remains in the on-state. For the estimated value of $F_2 = 0.123$, as we increase F_1 from 0, the system remains in the off-state until $F_1 = 0.01$, at which point the

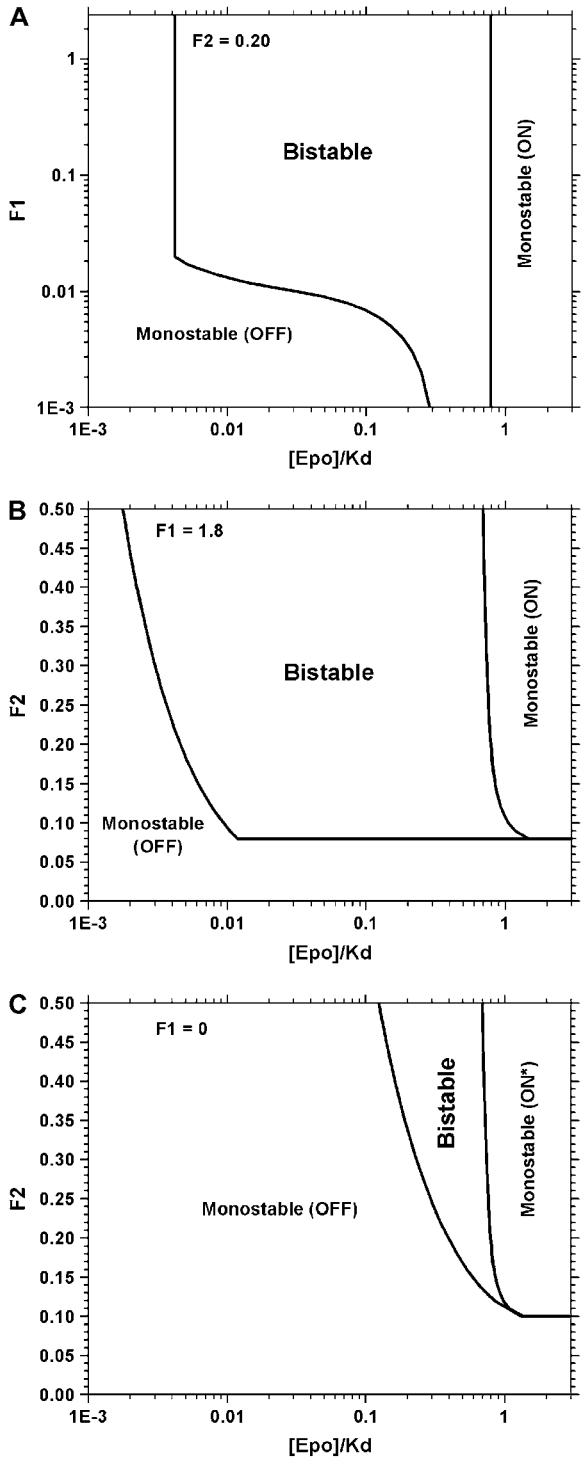

FIGURE 5 Bistable expression of GATA-1*. (*A*) A log-log plot showing the change in the bistable expression of GATA-1* for varying F_1 (F_2 = 0.20). The threshold Epo concentration needed to achieve the on-state appears to be independent of F_1. The maximum bistable window achievable is dependent on F_2; however, the width of the bistable window is F_1-dependent for lower F_1 values. (*B*) A semi-log plot showing the bistable expression of GATA-1* for changing F_2 values (F_1 = 1.8). There appears to be a threshold F_2 value below which the system is purely monostable. Increasing F_2 increases the width of the bistable window and, to a lesser extent, decreases the threshold Epo concentration required to reach the on-state. (*C*) Narrow bistable expression of GATA-1* for various F_2 values when F_1 = 0. The ON* state denotes an on-state due to activation but no accumulation. This state would not commit a cell to differentiate due to low basal levels of GATA-1. When F_2 = 0, the system is monostable for any F_1 value (e.g., the *x* axis in Fig. 5 *B*).

system switches to the on-state with a low GA set point value. As we further increase F_1 to 0.04, the system stays in the on-state and increases the GA steady-state value to the estimated value of 295. When F_1 is increased beyond 0.04, the steady-state value of GA increases and saturates at an F_1 value of 1.2.

A top view of the 3D plot is given in Fig. 4 *B* to address the effect of changes in F_1 and F_2 on the set point of GA in the on-state. In this phase diagram, the on-state is divided into two regions: F_1-limiting, where an increase in F_1 (but not F_2) will increase the set point of GA in the on-state, and F_2-limiting, where an increase in F_2 (but not F_1) will increase the set point of GA in the on-state. It can also be seen that the critical value of F_2 above which the system attains the on-state slightly decreases as we increase F_1 and the critical line eventually asymptotes at $F_2 = 0.05$ for very high F_1. The EpoR/GATA-1 system is likely to always be F_1-limited because of the extremely high GATA-1 levels required to be F_2-limited. Steady-state response plots of GA for several values of F_1 and F_2, spanning both F_1- and F_2-limited regions, are given in Fig. S5 (Data S1).

Bistable expression of GATA-1*

The steady-state response plot in Fig. 2 *D* shows the wide range of Epo concentrations in which GATA-1* exhibits bistable expression for the fitted F_1 and F_2 values. To understand the influence of the two positive feedback loops in defining the bistable window, we plotted the monostable (either ON or OFF) and bistable (ON and OFF) GATA-1* regions as a function of Epo concentration and feedback strength (Fig. 5). Here, the F_1 and F_2 values are chosen to cover both the F_1- and F_2-limiting regions as shown in Fig. 4 *B*. In Fig. 5 *A*, a log-log plot of F_1 versus [Epo]/K_d, with F_2 constant (0.20), shows the regions of monostable and bistable expression of GATA-1*. At low F_1 values, the system only achieves bistability for a narrow range of Epo concentrations. As we increase F_1, the bistable window increases and remains constant for larger F_1 values. The increase in the bistable window is only due to the decrease in the bistable-on to monostable-off transition concentration, as the bistable-off to monostable-on threshold concentration remains constant for all values of F_1. This reveals that the Epo concentration at which the system initially switches to the on-state is independent of F_1. However, F_1 governs the extent of memory in the system by changing the Epo concentration at which the system switches from the on-state to the off-state. Fig. 5 *B* shows a semilog plot of F_2 versus [Epo]/K_d, with F_1 constant (1.8). For values of F_2 <0.08, the system remains in the off-state for all Epo concentrations. The system attains the

on-state for higher F_2 values and also exhibits bistability for a wide range of Epo concentrations. In contrast to Fig. 5 *A*, the bistable window in Fig. 5 *B* shifts as we increase F_2 due to a substantial decrease in the bistable-on to monostable-off transition concentration as well as a smaller decrease in the bistable-off to monostable-on threshold concentration. This indicates that F_2 plays a role in determining the Epo concentration at which the system reaches on-state as well as in governing the magnitude of memory in the system.

Since basal levels of inactive GATA-1 are low, the system needs both F_1 (for accumulation of GATA-1) and F_2 (for activation of GATA-1) to attain the on-state (accumulation of activated GATA-1). For systems having a high basal expression level of inactive transcription factor or lineage-specific receptor (though neither is the case for the erythrocyte differentiation problem), it becomes relevant to examine how bistability may be achieved. Can such systems potentially attain the on-state* (activation, no accumulation) even if $F_1 = 0$ or $F_2 = 0$? We tested this using our EpoR/GATA-1 model, with F_1 fixed at 0. Fig. 5 *C* shows the bistable expression of the active transcription factor in the absence of F_1. For a given F_2, the Epo concentration at which the system attains the on-state does not change when compared with Fig. 5 *B*, but the respective concentration at which the system switches back to the monostable off-state is increased dramatically, thus narrowing the bistable window, or memory, in the system. A system that has feedback 1 (upregulation of GATA-1 by GATA-1*) but no feedback 2 (upregulation of EpoR by GATA-1*) does not exhibit bistability for any value of F_1, confirming the observation that autoregulating positive feedback loops without cooperativity do not show bistability in deterministic models (57,58); bistability in a system lacking feedback 2 can be recovered by incorporating the need for transcription factor dimerization for activation (data not shown). In summary, this shows that the bistability and ultrasensitivity achieved in the EpoR/GATA-1 model were primarily due to the presence of feedback 2, and that feedback 1 only plays a role in increasing the extent of memory in the system. The values of F_1 and F_2 may also change during the differentiation process, thus dynamically modulating the robustness of the system, though this time dependence was not considered here.

Construction of a generalized minimal model

The EpoR/GATA-1 model exhibits ultrasensitivity and bistability for a wide range of Epo, F_1, and F_2 values. The structural aspects of the EpoR/GATA-1 model are the two linked positive feedback loops, receptor homodimerization, PI3K/AKT signaling pathway, double phosphorylation of AKT, and the transcription and translation steps. We systematically developed and tested various submodels of the parent model to identify the dispensable steps and to obtain a generalized minimal model that still retains the ultrasensitivity and robust bistability of the parent model (data not shown). This analysis revealed that the two positive feedback loops were both necessary and sufficient for recapitulating the overall system behavior of the full EpoR/GATA-1 model. This reduced lineage-specific receptor/transcription factor model (Fig. 6) includes only four time-dependent species: receptor (R), complex (C), and inactive (ITF) and active (ATF) transcription factor. This model was solved analytically and the exact solution for each of the four reactants was determined (Table S11, Data S1). The steady-state response plots for these reactants for selected values of F_1 and F_2 are given in Fig. S6 (Data S1). The bistability plots of ATF (Fig. S7, Data S1) in the minimal model closely mimic those in the EpoR/GATA-1 model (Fig. 5).

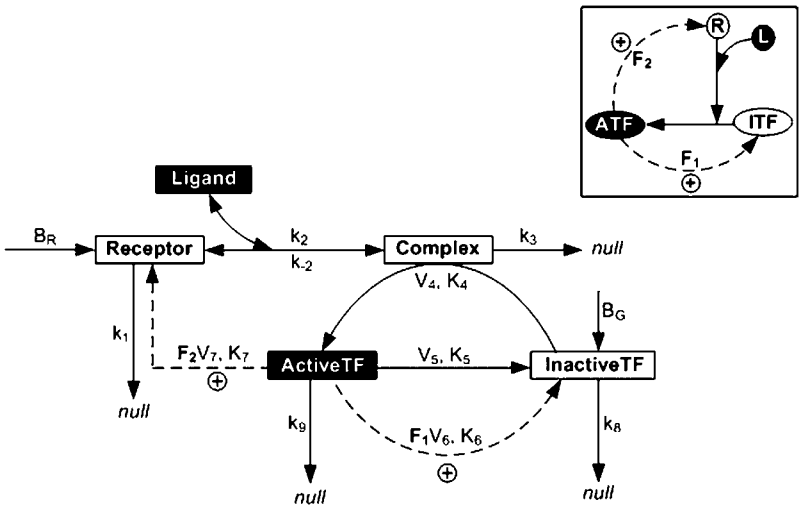

FIGURE 6 Generalized minimal model for lineage commitment. Receptor and Inactive Transcription Factor (InactiveTF) are present at basal levels before the addition of ligand. Ligand binds to Receptor to form Complex and activates InactiveTF to form Active Transcription Factor (ActiveTF). ActiveTF upregulates the levels of InactiveTF and Receptor through two positive feedback loops. Reaction sets (1–3, 8, and 9), (4 and 5), and (6 and 7) are modeled with mass-action, Michaelis-Menten, and rapid-equilibrium kinetics, respectively. Double-headed and single-headed solid arrows indicate reversible and irreversible reactions, respectively. Dashed arrows specify irreversible transcriptional activation and translation reactions (modeled as a single step). All reactants except ligand are time variant. All reactions going to *null* denote first-order degradation processes. The values of the rate constants shown in the figure are given in Table S12 (Data S1). (*Inset*) A further simplified schematic of the minimal model highlighting the two feedback loops. L, R, ITF, and ATF denote the nondimensional forms of Ligand, Receptor, InactiveTF, and ActiveTF, respectively. Basally expressed R converts basally expressed ITF to ATF only in the presence of L. ATF upregulates itself by inducing the expression of both ITF (with transcriptional strength F_1) and R (with transcriptional strength F_2). It should be noted that positive feedback to ITF is intrinsically regulated, whereas positive feedback via R (to activate ITF) is dependent on the external stimulus L.

Bifurcation analysis of the minimal model

Unlike the EpoR/GATA-1 model, the minimal model can be solved analytically, which can prove useful in understanding the contributions of each of the two positive feedback loops to the overall behavior of the system. The solution curves of ATF are plotted against L (normalized to its K_d) for various values of F_2 holding F_1 constant at 20 as shown in Fig. 7 *A*. The solid lines and the dotted lines denote the stable and unstable roots, respectively. For low values of F_2 (0.01), the system has only two real roots (one stable and one unstable) and is purely monostable for all ligand concentrations. As F_2 is increased to 0.1, the expression of the ActiveTF becomes narrowly bistable, with the endpoints of this bistable

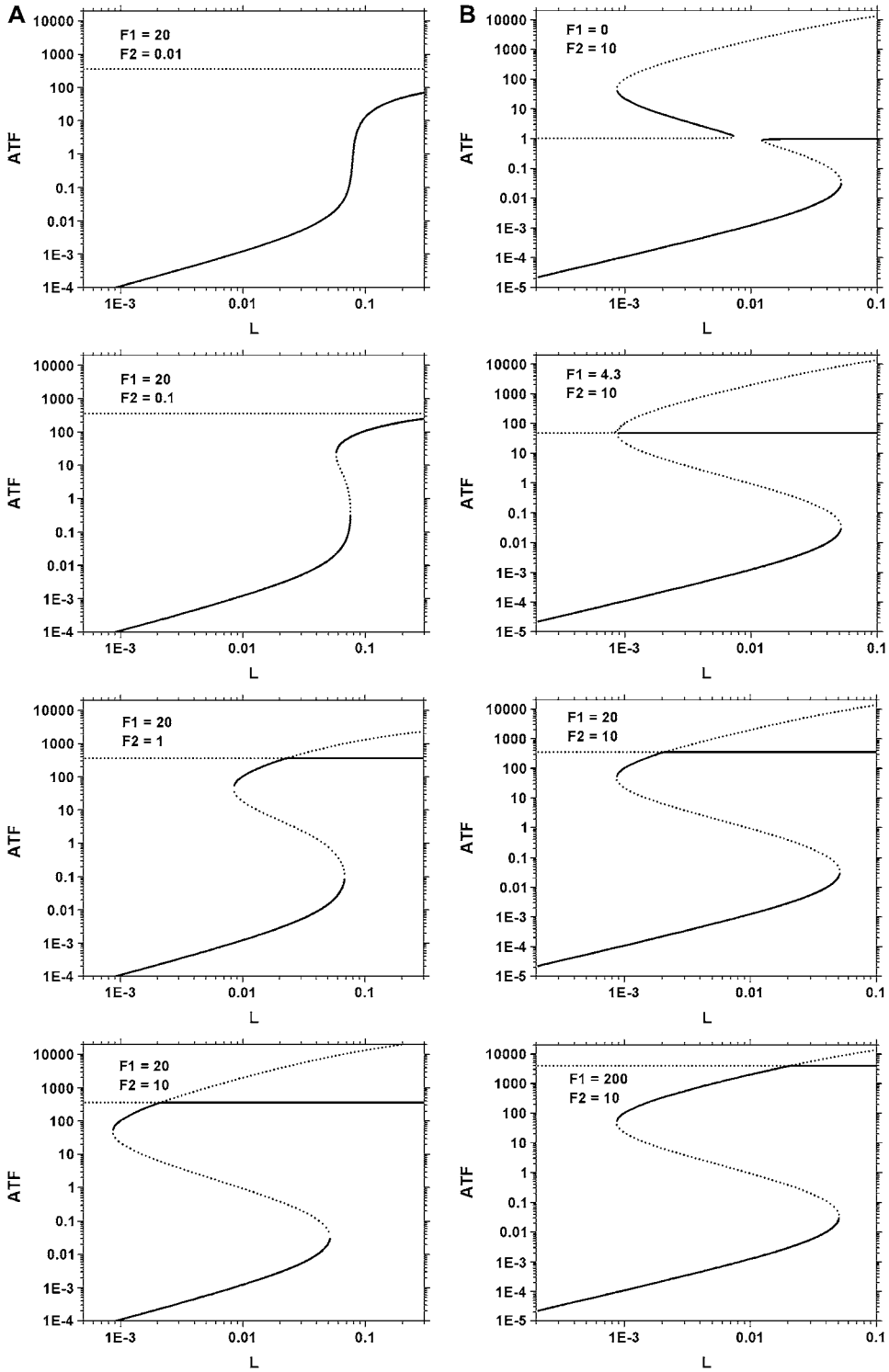

FIGURE 7 Bifurcation analysis for the minimal model. (*A*) Solution curves obtained from the analytical solution of nondimensionalized Active Transcription Factor (ATF) are plotted against ligand concentration normalized to its K_d (L) by varying F_2 (0.01, 0.1, 1, and 10); F_1 is held constant at 20. The solid lines and the dotted lines denote the stable and unstable roots, respectively. For low F_2 values, the system is purely monostable. As we increase F_2, two saddle-node bifurcations emerge and they determine the width of the bistable window and the threshold ligand concentration necessary to reach the on-state. As we further increase F_2, the solution curves intersect to form a transcritical bifurcation. The saddle-node set points and the transcritical set point (maximum achievable on-state value) are F_2- and F_1-dependent, respectively. (*B*) F_1 is varied (0, 4.3, 20, and 200); F_2 is held constant at 10. The system can achieve bistable expression of ATF even when $F_1 = 0$. As we increase F_1, the bistable window increases and reaches a maximum width, which is determined only by the F_2 value. Increasing F_1 further increases the on-state set point value of ATF but has no effect on the threshold ligand concentration required to reach the on-state.

window defined by two saddle-node bifurcations that appear to depend on F_2 but not on F_1 (see below). The degree of bistability increases dramatically as F_2 is increased to 1 and then to 10. It can be seen that, for these larger F_2 values, the solution curves intersect to form a transcritical bifurcation. The transcritical set point, which constrains the maximum theoretical value of ATF, seems to be independent of F_2. The transcritical bifurcation also divides the bistable window into F_1-limiting (right of the transcritical bifurcation point; constant on-state value) and F_2-limiting regions (left of the transcritical bifurcation point; variable on-state value). For low F_2 values, the bistable region is completely F_2-limited and as we increase F_2, the bistable region becomes increasingly F_1-limited. Finally, it can also be observed that the threshold ligand concentration to achieve the on-state decreases as we increase the F_2 value.

Fig. 7 *B* shows the bifurcation diagrams for ATF plotted against L by varying F_1 and keeping F_2 constant at 10. Unlike the previous case (Fig. 7 *A*), the system can achieve bistability over a narrow range of L by forming two saddle-node bifurcations even when F_1 is zero. As we increase F_1, the size of the bistable window and the on-state set point value both increase. At a critical value of F_1 (here 4.3), the maximum bistable window is achieved, coincident with the appearance of an apparent subcritical pitchfork bifurcation at the lowest value of L at which the system is still bistable. At this F_1 value, the set point of the ATF in the bistable region is completely F_1-limited. As F_1 is increased beyond 4.3, the solution curves form a transcritical bifurcation similar to that seen in Fig. 7 *A*. As we further raise the value of F_1 to 20 and then 200, the value of L at which the transcritical bifurcation occurs shifts from low to high, making the bistable region increasingly F_2-limited. This is in contrast to Fig. 7 *A*, where the transcritical bifurcation point moves from right to left and the bistable region becomes increasingly F_1-limited as we increase F_2. Importantly, increasing F_1 augments the maximum on-state set point value of ATF but has no effect on the threshold ligand concentration necessary for achieving the on-state.

By comparing the bifurcation plots of ATF in Fig. 7 with various plots of activated GATA-1 (Fig. 2 *D*, Fig. 5, and Fig. S5 in Data S1), the following conclusions can be deduced for the EpoR/GATA-1 system: the width of the bistable region and the range of GATA-1* values in the on-state can both depend on F_1 (under F_1-limited conditions) and/or F_2 (under F_2-limited conditions); the maximum GATA-1* value in the on-state is determined by F_1; the threshold Epo concentration at which the system switches to the on-state is dictated by F_2; the maximum bistable window achievable is set by F_2; and, the system requires an F_2 value above a critical threshold to exhibit bistability.

DISCUSSION

EpoR and GATA-1 are both essential for erythrocyte precursor commitment and differentiation, and we present here a deterministic model that bidirectionally links the lineage-specific receptor and transcription factor. Based on recent biochemical data (42,43,45,53), we chose the PI3K/AKT cascade as the signaling pathway that connects EpoR and GATA-1. The model accounts for basal expression of EpoR and GATA-1, Epo binding to EpoR to activate the PI3K/AKT pathway, activation of GATA-1 by phosphorylated AKT, positive autoregulation of GATA-1 expression by GATA-1*, and upregulation of EpoR expression by GATA-1*.

To gain mechanistic insights into system behavior, we chose to focus on this small set of critical molecular effectors implicated in erythropoiesis. However, it should be noted that our explicitly modeled topology represents only a fraction of the full regulatory network and, therefore, inferring cell fate from the level of a single metric (e.g., GATA-1*) represents an approximation of a high-dimensional attractor (55,73). Signaling pathways that were excluded from our model include JAK2/STAT5/Bcl_{XL}, which provides antiapoptotic signals during erythrocyte differentiation (74), and Ras/MAPK, which is involved in cell survival (75), cell-cycle regulation (76), and the degradation of DNA-bound GATA-1 (77). Also, the JAK2/STAT5 pathway activated by Epo can initiate a negative feedback loop on the PI3K/AKT pathway by activating SOCS proteins that can suppress Epo receptor signaling (78,79). Our model, despite neglecting these additional complexities, can nevertheless effectively capture the system dynamics observed in multiple indepedent experimental data sets (see Fig. S1, Data S1).

Through steady-state response plots (Fig. 2) and bistability plots (Fig. 5), it was revealed that the EpoR/GATA-1 network can exhibit ultrasensitivity and bistability. Since these properties may play important roles in erythrocyte commitment, it was informative to probe the role of positive feedback in such a topology. As shown in Fig. 7 *A*, positive receptor feedback can ultrasensitize the system to ligand and can generate a considerable memory effect once the on-state is achieved. Other transcription factors (e.g., GATA-3 (80)) are believed to be intracellularly amplified through a classical autoregulatory positive feedback loop: synthesis of the new transcription factor is followed by dimerization (or higher order oligomerization) and the complex is then transcriptionally active. If this is sufficient for programming cell fate, why, then, might a transcription factor such as GATA-1 have evolved to upregulate a lineage-specific receptor as well?

The answer may lie in the different modes of activation. Whereas the dimerization step closes the positive feedback loop for some transcription factors, experimental evidence suggests that GATA-1 binds DNA as a monomer (34,81,82) and shows no detectable DNA-binding ability before the addition of Epo (41). Thus, EpoR signaling may be necessary to close the GATA-1 autoregulatory loop by activating the transcription factor via AKT. By upregulating EpoR to increase its own activation, GATA-1 can effectively mimic the molecular cooperativity of other transcription factors in generating robust network bistability without employing any

cooperative reactions. (The importance of cooperativity in achieving bistability is restricted to the class of deterministic models discussed in this work; it is indeed possible to achieve steep sigmoidal responses through nonidealities such as molecular crowding (83), stochastic focusing (84), and dimensionally restricted reactions (63).)

Two unique elements of the EpoR/GATA-1 model should be highlighted. First, by decoupling the synthesis and activation steps in the positive GATA-1 autoregulatory loop, a cell may be able to independently tune the switching threshold, the on-state expression level, and the extent of memory in the network by separately modulating F_1 and F_2 (e.g., epigenetically). Second, there is an external checkpoint (Epo) that modulates this autoregulatory loop. This is attractive because it provides a novel and meaningful link between canonically extrinsic (cytokine) and intrinsic (transcription factor) signals in regulating not only cell survival but also maturation.

The strengths of the positive feedback loops are governed by the rates of transcription of *GATA1* (F_1) and *EPOR* (F_2). The estimated values of F_1 and F_2 are 0.04 and 0.123, respectively. The difference in the rates of transcription of *EPOR* (chromosome 19p13.2) and *GATA1* (chromosome Xp11.23) may be due to the distinct binding mechanisms of GATA-1 to these promoters, dissimilarities in the ease of accession of the GATA-1 binding sites, and the recruitment of other cofactors that may regulate *EPOR* and *GATA1* expression differently. GATA-1 also interacts with other factors, notably the ubiquitous transcription factor Sp1, erythroid restricted factor EKLF, and friend of GATA-1 (FOG1) that may alter its transcriptional activity among the various GATA-1 regulated genes (29).

Though treated as constants in our model, F_1 and F_2 may also change temporally during commitment and differentiation due to additional biophysical (e.g., chromatin remodeling) and biochemical (e.g., cofactor upregulation/downregulation) processes. Accordingly, the values of F_1 and F_2 may also vary substantially between primary cells and immortalized lines, and may even differ among cell lines, depending upon how far a cell line is from commitment toward the erythrocyte lineage, relative expression of GATA-1 cofactors, basal levels of EpoR and GATA-1 expression, and expression of antagonistic transcription factors driving other lineages. Cell-specific feedback strengths that differ significantly from those used in our models may serve to attenuate or amplify the actual effects on the network.

Finally, system-level properties such as bistability and ultrasensitivity that may be generally applicable to lineage commitment can be experimentally corroborated. Pretreatment of progenitor cells with ligand, as outlined in the Results section (Fig. 3), can be performed to show expected hystereses in transcription factor activation and lineage commitment. Additionally, the models elucidate how the steady-state response profiles of activated transcription factor can be influenced by F_1 and F_2, and these can be experimentally validated by using pharmacological inhibitors or RNA interference to exogenously manipulate the values of F_1 and F_2. Although the results presented here are motivated by the EpoR/GATA-1 network and its critical role in erythropoiesis, it will be interesting to see whether similar topologies are uncovered in other cell systems that enable their hosts to make robust decisions in response to external stimuli.

SUPPLEMENTARY MATERIAL

To view all of the supplemental files associated with this article, visit www.biophysj.org.

We are grateful to Mitchell Weiss and Harvey Lodish for lending their expertise in erythropoiesis. We also thank Anand Asthagiri and an anonymous reviewer for very helpful suggestions.

This work was supported by startup funds from the University of Pennsylvania to C.A.S.

REFERENCES

1. Ferrell, J. E., and W. Xiong. 2001. Bistability in cell signaling: How to make continuous processes discontinuous, and reversible processes irreversible. *Chaos.* 11:227–236.
2. Ferrell, J. E., Jr., and E. M. Machleder. 1998. The biochemical basis of an all-or-none cell fate switch in *Xenopus* oocytes. *Science.* 280:895–898.
3. Cross, F. R., V. Archambault, M. Miller, and M. Klovstad. 2002. Testing a mathematical model of the yeast cell cycle. *Mol. Biol. Cell.* 13:52–70.
4. Xiong, W., and J. E. Ferrell Jr. 2003. A positive-feedback-based bistable 'memory module' that governs a cell fate decision. *Nature.* 426:460–465.
5. Gardner, T. S., C. R. Cantor, and J. J. Collins. 2000. Construction of a genetic toggle switch in *Escherichia coli*. *Nature.* 403:339–342.
6. Hasty, J., J. Pradines, M. Dolnik, and J. J. Collins. 2000. Noise-based switches and amplifiers for gene expression. *Proc. Natl. Acad. Sci. USA.* 97:2075–2080.
7. Samoilov, M., S. Plyasunov, and A. P. Arkin. 2005. Stochastic amplification and signaling in enzymatic futile cycles through noise-induced bistability with oscillations. *Proc. Natl. Acad. Sci. USA.* 102: 2310–2315.
8. Rosenfeld, N., J. W. Young, U. Alon, P. S. Swain, and M. B. Elowitz. 2005. Gene regulation at the single-cell level. *Science.* 307:1962–1965.
9. Rosenfeld, N., and U. Alon. 2003. Response delays and the structure of transcription networks. *J. Mol. Biol.* 329:645–654.
10. Laslo, P., C. J. Spooner, A. Warmflash, D. W. Lancki, H. J. Lee, R. Sciammas, B. N. Gantner, A. R. Dinner, and H. Singh. 2006. Multilineage transcriptional priming and determination of alternate hematopoietic cell fates. *Cell.* 126:755–766.
11. Legewie, S., N. Bluthgen, R. Schafer, and H. Herzel. 2005. Ultrasensitization: switch-like regulation of cellular signaling by transcriptional induction. *PLoS Comput. Biol.* 1:e54.
12. Goldbeter, A., and D. E. Koshland Jr. 1982. Sensitivity amplification in biochemical systems. *Q. Rev. Biophys.* 15:555–591.
13. Koshland, D. E., Jr., A. Goldbeter, and J. B. Stock. 1982. Amplification and adaptation in regulatory and sensory systems. *Science.* 217: 220–225.
14. Chang, H. H., P. Y. Oh, D. E. Ingber, and S. Huang. 2006. Multistable and multistep dynamics in neutrophil differentiation. *BMC Cell Biol.* 7:11.
15. Metcalf, D. 1998. Lineage commitment and maturation in hematopoietic cells: the case for extrinsic regulation. *Blood.* 92:345–347 (discussion 352).

16. Enver, T., C. M. Heyworth, and T. M. Dexter. 1998. Do stem cells play dice? *Blood.* 92:348–351 (discussion 352).

17. Krantz, S. B. 1991. Erythropoietin. *Blood.* 77:419–434.

18. D'Andrea, A. D., G. D. Fasman, and H. F. Lodish. 1989. Erythropoietin receptor and interleukin-2 receptor beta chain: a new receptor family. *Cell.* 58:1023–1024.

19. Lu, X., A. W. Gross, and H. F. Lodish. 2006. Active conformation of the erythropoietin receptor: random and cysteine-scanning mutagenesis of the extracellular juxtamembrane and transmembrane domains. *J. Biol. Chem.* 281:7002–7011.

20. Constantinescu, S. N., S. Ghaffari, and H. F. Lodish. 1999. The erythropoietin receptor: structure, activation and intracellular signal transduction. *Trends Endocrinol. Metab.* 10:18–23.

21. Ghaffari, S., C. Kitidis, M. D. Fleming, H. Neubauer, K. Pfeffer, and H. F. Lodish. 2001. Erythropoiesis in the absence of janus-kinase 2: BCR-ABL induces red cell formation in JAK2(−/−) hematopoietic progenitors. *Blood.* 98:2948–2957.

22. Wu, H., X. Liu, R. Jaenisch, and H. F. Lodish. 1995. Generation of committed erythroid BFU-E and CFU-E progenitors does not require erythropoietin or the erythropoietin receptor. *Cell.* 83:59–67.

23. Evans, T., and G. Felsenfeld. 1989. The erythroid-specific transcription factor Eryf1: a new finger protein. *Cell.* 58:877–885.

24. Martin, D. I., and S. H. Orkin. 1990. Transcriptional activation and DNA binding by the erythroid factor GF-1/NF-E1/Eryf 1. *Genes Dev.* 4:1886–1898.

25. Welch, J. J., J. A. Watts, C. R. Vakoc, Y. Yao, H. Wang, R. C. Hardison, G. A. Blobel, L. A. Chodosh, and M. J. Weiss. 2004. Global regulation of erythroid gene expression by transcription factor GATA-1. *Blood.* 104:3136–3147.

26. Orkin, S. H. 1990. Globin gene regulation and switching: circa 1990. *Cell.* 63:665–672.

27. Mignotte, V., J. F. Eleouet, N. Raich, and P. H. Romeo. 1989. Cis- and trans-acting elements involved in the regulation of the erythroid promoter of the human porphobilinogen deaminase gene. *Proc. Natl. Acad. Sci. USA.* 86:6548–6552.

28. Cantor, A. B., and S. H. Orkin. 2002. Transcriptional regulation of erythropoiesis: an affair involving multiple partners. *Oncogene.* 21: 3368–3376.

29. Tang, X. B., D. P. Liu, and C. C. Liang. 2001. Regulation of the transcription factor GATA-1 at the gene and protein level. *Cell. Mol. Life Sci.* 58:2008–2017.

30. Chiba, T., Y. Ikawa, and K. Todokoro. 1991. GATA-1 transactivates erythropoietin receptor gene, and erythropoietin receptor-mediated signals enhance GATA-1 gene expression. *Nucleic Acids Res.* 19: 3843–3848.

31. Kuramochi, S., Y. Ikawa, and K. Todokoro. 1990. Characterization of murine erythropoietin receptor genes. *J. Mol. Biol.* 216:567–575.

32. Zon, L. I., H. Youssoufian, C. Mather, H. F. Lodish, and S. H. Orkin. 1991. Activation of the erythropoietin receptor promoter by transcription factor GATA-1. *Proc. Natl. Acad. Sci. USA.* 88:10638–10641.

33. Hannon, R., T. Evans, G. Felsenfeld, and H. Gould. 1991. Structure and promoter activity of the gene for the erythroid transcription factor GATA-1. *Proc. Natl. Acad. Sci. USA.* 88:3004–3008.

34. Tsai, S. F., E. Strauss, and S. H. Orkin. 1991. Functional analysis and in vivo footprinting implicate the erythroid transcription factor GATA-1 as a positive regulator of its own promoter. *Genes Dev.* 5:919–931.

35. Zon, L. I., and S. H. Orkin. 1992. Sequence of the human GATA-1 promoter. *Nucleic Acids Res.* 20:1812.

36. Iwasaki, H., S. Mizuno, R. A. Wells, A. B. Cantor, S. Watanabe, and K. Akashi. 2003. GATA-1 converts lymphoid and myelomonocytic progenitors into the megakaryocyte/erythrocyte lineages. *Immunity.* 19: 451–462.

37. Pevny, L., M. C. Simon, E. Robertson, W. H. Klein, S. F. Tsai, V. D'Agati, S. H. Orkin, and F. Costantini. 1991. Erythroid differentiation in chimaeric mice blocked by a targeted mutation in the gene for transcription factor GATA-1. *Nature.* 349:257–260.

38. Wickrema, A., S. B. Krantz, J. C. Winkelmann, and M. C. Bondurant. 1992. Differentiation and erythropoietin receptor gene expression in human erythroid progenitor cells. *Blood.* 80:1940–1949.

39. Fibach, E., D. Manor, A. Oppenheim, and E. A. Rachmilewitz. 1989. Proliferation and maturation of human erythroid progenitors in liquid culture. *Blood.* 73:100–103.

40. Broudy, V. C., N. Lin, M. Brice, B. Nakamoto, and T. Papayannopoulou. 1991. Erythropoietin receptor characteristics on primary human erythroid cells. *Blood.* 77:2583–2590.

41. Dalyot, N., E. Fibach, A. Ronchi, E. A. Rachmilewitz, S. Ottolenghi, and A. Oppenheim. 1993. Erythropoietin triggers a burst of GATA-1 in normal human erythroid cells differentiating in tissue culture. *Nucleic Acids Res.* 21:4031–4037.

42. Zhao, W., C. Kitidis, M. D. Fleming, H. F. Lodish, and S. Ghaffari. 2006. Erythropoietin stimulates phosphorylation and activation of GATA-1 via the PI3-kinase/AKT signaling pathway. *Blood.* 107: 907–915.

43. Ghaffari, S., C. Kitidis, W. Zhao, D. Marinkovic, M. D. Fleming, B. Luo, J. Marszalek, and H. F. Lodish. 2006. AKT induces erythroid-cell maturation of JAK2-deficient fetal liver progenitor cells and is required for Epo regulation of erythroid-cell differentiation. *Blood.* 107:1888–1891.

44. Rooke, H. M., and S. H. Orkin. 2006. Phosphorylation of Gata1 at serine residues 72, 142, and 310 is not essential for hematopoiesis in vivo. *Blood.* 107:3527–3530.

45. Blobel, G. A., T. Nakajima, R. Eckner, M. Montminy, and S. H. Orkin. 1998. CREB-binding protein cooperates with transcription factor GATA-1 and is required for erythroid differentiation. *Proc. Natl. Acad. Sci. USA.* 95:2061–2066.

46. Boyes, J., P. Byfield, Y. Nakatani, and V. Ogryzko. 1998. Regulation of activity of the transcription factor GATA-1 by acetylation. *Nature.* 396:594–598.

47. Hung, H. L., J. Lau, A. Y. Kim, M. J. Weiss, and G. A. Blobel. 1999. CREB-Binding protein acetylates hematopoietic transcription factor GATA-1 at functionally important sites. *Mol. Cell. Biol.* 19:3496–3505.

48. Lamonica, J. M., C. R. Vakoc, and G. A. Blobel. 2006. Acetylation of GATA-1 is required for chromatin occupancy. *Blood.* 108:3736–3738.

49. Blobel, G. A. 2000. CREB-binding protein and p300: molecular integrators of hematopoietic transcription. *Blood.* 95:745–755.

50. Letting, D. L., C. Rakowski, M. J. Weiss, and G. A. Blobel. 2003. Formation of a tissue-specific histone acetylation pattern by the hematopoietic transcription factor GATA-1. *Mol. Cell. Biol.* 23:1334–1340.

51. Liu, Y., C. E. Denlinger, B. K. Rundall, P. W. Smith, and D. R. Jones. 2006. Suberoylanilide hydroxamic acid induces Akt-mediated phosphorylation of p300, which promotes acetylation and transcriptional activation of RelA/p65. *J. Biol. Chem.* 281:31359–31368.

52. Vojtek, A. B., J. Taylor, S. L. DeRuiter, J. Y. Yu, C. Figueroa, R. P. Kwok, and D. L. Turner. 2003. Akt regulates basic helix-loop-helix transcription factor-coactivator complex formation and activity during neuronal differentiation. *Mol. Cell. Biol.* 23:4417–4427.

53. Huang, W. C., and C. C. Chen. 2005. Akt phosphorylation of p300 at Ser-1834 is essential for its histone acetyltransferase and transcriptional activity. *Mol. Cell. Biol.* 25:6592–6602.

54. Roeder, I., and I. Glauche. 2006. Towards an understanding of lineage specification in hematopoietic stem cells: a mathematical model for the interaction of transcription factors GATA-1 and PU.1. *J. Theor. Biol.* 241:852–865.

55. Huang, S., Y. P. Guo, G. May, and T. Enver. 2007. Bifurcation dynamics in lineage-commitment in bipotent progenitor cells. *Dev. Biol.* 305:695–713.

56. Ortega, F., J. L. Garces, F. Mas, B. N. Kholodenko, and M. Cascante. 2006. Bistability from double phosphorylation in signal transduction. Kinetic and structural requirements. *FEBS J.* 273:3915–3926.

57. Angeli, D., J. E. Ferrell Jr., and E. D. Sontag. 2004. Detection of multistability, bifurcations, and hysteresis in a large class of biological positive-feedback systems. *Proc. Natl. Acad. Sci. USA.* 101:1822–1827.

58. Muzzey, D., and A. van Oudenaarden. 2006. When it comes to decisions, myeloid progenitors crave positive feedback. *Cell.* 126:650–652.

59. Lai, K., M. J. Robertson, and D. V. Schaffer. 2004. The sonic hedgehog signaling system as a bistable genetic switch. *Biophys. J.* 86:2748–2757.

60. Ferrell, J. E., Jr. 2002. Self-perpetuating states in signal transduction: positive feedback, double-negative feedback and bistability. *Curr. Opin. Cell Biol.* 14:140–148.

61. Huang, C. Y., and J. E. Ferrell Jr. 1996. Ultrasensitivity in the mitogen-activated protein kinase cascade. *Proc. Natl. Acad. Sci. USA.* 93:10078–10083.

62. Bhalla, U. S., and R. Iyengar. 2001. Robustness of the bistable behavior of a biological signaling feedback loop. *Chaos.* 11:221–226.

63. Savageau, M. A. 1995. Michaelis-Menten mechanism reconsidered: implications of fractal kinetics. *J. Theor. Biol.* 176:115–124.

64. Callard, R. E., and A. J. Yates. 2005. Immunology and mathematics: crossing the divide. *Immunology.* 115:21–33.

65. Hatakeyama, M., S. Kimura, T. Naka, T. Kawasaki, N. Yumoto, M. Ichikawa, J. H. Kim, K. Saito, M. Saeki, M. Shirouzu, S. Yokoyama, and A. Konagaya. 2003. A computational model on the modulation of mitogen-activated protein kinase (MAPK) and Akt pathways in heregulin-induced ErbB signalling. *Biochem. J.* 373:451–463.

66. Alessi, D. R., S. R. James, C. P. Downes, A. B. Holmes, P. R. Gaffney, C. B. Reese, and P. Cohen. 1997. Characterization of a 3-phosphoinositide-dependent protein kinase which phosphorylates and activates protein kinase Balpha. *Curr. Biol.* 7:261–269.

67. Andjelkovic, M., S. M. Maira, P. Cron, P. J. Parker, and B. A. Hemmings. 1999. Domain swapping used to investigate the mechanism of protein kinase B regulation by 3-phosphoinositide-dependent protein kinase 1 and Ser473 kinase. *Mol. Cell. Biol.* 19:5061–5072.

68. Smolen, P., D. A. Baxter, and J. H. Byrne. 1998. Frequency selectivity, multistability, and oscillations emerge from models of genetic regulatory systems. *Am. J. Physiol.* 274:C531–C542.

69. Yamada, S., S. Shiono, A. Joo, and A. Yoshimura. 2003. Control mechanism of JAK/STAT signal transduction pathway. *FEBS Lett.* 534:190–196.

70. Schmidt, H., and M. Jirstrand. 2006. Systems Biology Toolbox for MATLAB: a computational platform for research in systems biology. *Bioinformatics.* 22:514–515.

71. Keller, M. A., S. Addya, R. Vadigepalli, B. Banini, K. Delgrosso, H. Huang, and S. Surrey. 2006. Transcriptional regulatory network analysis of developing human erythroid progenitors reveals patterns of coregulation and potential transcriptional regulators. *Physiol. Genomics.* 28: 114–128.

72. Gross, A. W., and H. F. Lodish. 2006. Cellular trafficking and degradation of erythropoietin and novel erythropoiesis stimulating protein (NESP). *J. Biol. Chem.* 281:2024–2032.

73. Huang, S., G. Eichler, Y. Bar-Yam, and D. E. Ingber. 2005. Cell fates as high-dimensional attractor states of a complex gene regulatory network. *Phys. Rev. Lett.* 94:128701.

74. Battle, T. E., and D. A. Frank. 2002. The role of STATs in apoptosis. *Curr. Mol. Med.* 2:381–392.

75. Yu, Y. L., Y. J. Chiang, Y. C. Chen, M. Papetti, C. G. Juo, A. I. Skoultchi, and J. J. Yen. 2005. MAPK-mediated phosphorylation of GATA-1 promotes Bcl-XL expression and cell survival. *J. Biol. Chem.* 280:29533–29542.

76. Richmond, T. D., M. Chohan, and D. L. Barber. 2005. Turning cells red: signal transduction mediated by erythropoietin. *Trends Cell Biol.* 15:146–155.

77. Hernandez-Hernandez, A., P. Ray, G. Litos, M. Ciro, S. Ottolenghi, H. Beug, and J. Boyes. 2006. Acetylation and MAPK phosphorylation cooperate to regulate the degradation of active GATA-1. *EMBO J.* 25: 3264–3274.

78. Starr, R., T. A. Willson, E. M. Viney, L. J. Murray, J. R. Rayner, B. J. Jenkins, T. J. Gonda, W. S. Alexander, D. Metcalf, N. A. Nicola, and D. J. Hilton. 1997. A family of cytokine-inducible inhibitors of signalling. *Nature.* 387:917–921.

79. Endo, T. A., M. Masuhara, M. Yokouchi, R. Suzuki, H. Sakamoto, K. Mitsui, A. Matsumoto, S. Tanimura, M. Ohtsubo, H. Misawa, T. Miyazaki, N. Leonor, T. Taniguchi, T. Fujita, Y. Kanakura, S. Komiya, and A. Yoshimura. 1997. A new protein containing an SH2 domain that inhibits JAK kinases. *Nature.* 387:921–924.

80. Hofer, T., H. Nathansen, M. Lohning, A. Radbruch, and R. Heinrich. 2002. GATA-3 transcriptional imprinting in Th2 lymphocytes: a mathematical model. *Proc. Natl. Acad. Sci. USA.* 99:9364–9368.

81. Nalefski, E. A., E. Nebelitsky, J. A. Lloyd, and S. R. Gullans. 2006. Single-molecule detection of transcription factor binding to DNA in real time: specificity, equilibrium, and kinetic parameters. *Biochemistry.* 45:13794–13806.

82. Omichinski, J. G., G. M. Clore, O. Schaad, G. Felsenfeld, C. Trainor, E. Appella, S. J. Stahl, and A. M. Gronenborn. 1993. NMR structure of a specific DNA complex of Zn-containing DNA binding domain of GATA-1. *Science.* 261:438–446.

83. Savageau, M. A. 1993. Influence of fractal kinetics on molecular recognition. *J. Mol. Recognit.* 6:149–157.

84. Paulsson, J., O. G. Berg, and M. Ehrenberg. 2000. Stochastic focusing: fluctuation-enhanced sensitivity of intracellular regulation. *Proc. Natl. Acad. Sci. USA.* 97:7148–7153.